

Surface Extended-X-Ray-Absorption Fine Structure and Scanning Tunneling Microscopy of Si(001)2×1-Sb

M. Richter,⁽¹⁾ J. C. Woicik,⁽²⁾ J. Nogami,⁽³⁾ P. Pianetta,⁽¹⁾ K. E. Miyano,⁽⁴⁾ A. A. Baski,⁽³⁾
T. Kendelewicz,⁽⁴⁾ C. E. Bouldin,⁽²⁾ W. E. Spicer,⁽⁴⁾ C. F. Quate,⁽³⁾ and I. Lindau⁽¹⁾

⁽¹⁾Stanford Synchrotron Radiation Laboratory, Stanford, California 94309

⁽²⁾National Institute of Standards and Technology, Gaithersburg, Maryland 20899

⁽³⁾Edward L. Ginzton Laboratory, Stanford, California 94305

⁽⁴⁾Stanford Electronics Laboratory, Stanford, California 94305

(Received 10 September 1990)

Surface extended-x-ray-absorption fine structure (SEXAFS) has been combined with scanning tunneling microscopy (STM) to determine both the local and long-range bonding properties of the Si(001)2×1-Sb interface. Sb L_3 edge SEXAFS shows that Sb dimers occupy a modified bridge site on the Si(001) surface with a Sb-Sb near-neighbor distance of 2.88 ± 0.03 Å. Each Sb atom of the dimer is bonded to two Si atoms with a Sb-Si bond length of 2.63 ± 0.04 Å. STM resolves the dimer structure and provides the long-range periodicity of the surface. Low-energy-electron diffraction of vicinal Si(001) shows that the Sb dimer chains run perpendicular to the original Si dimer chains.

PACS numbers: 61.10.Lx, 61.16.Di

Since its invention in 1982,¹ scanning tunneling microscopy (STM) has proven to be a valuable real-space surface probe capable of atomic resolution. Although STM can provide images of surfaces with lateral resolution on the order of 3 Å, these images can be interpreted easily only in the most simple cases. For example, the structure of the Sb-GaAs(110) surface was solved only by comparing STM images with structures derived from low-energy-electron diffraction (LEED).² It is also often the case that only groups of atoms are resolved as a single feature in an STM image, as in a recent study of the As-terminated GaAs($\bar{1}\bar{1}\bar{1}$) surface.³ Although STM can provide long-range periodicity, it requires additional information to determine the true surface structure on an atomic scale.

Surface extended-x-ray-absorption fine structure (SEXAFS) is a proven technique for surface structure determination.⁴ It has the ability to measure near-neighbor bond lengths to an accuracy of 0.02 Å. SEXAFS can also determine adatom-substrate registry and coordination that, when combined with the symmetry information obtained from LEED, can lead to an unambiguous determination of the adsorption site geometry. The drawbacks of SEXAFS are that it determines only short-range order, and it is applicable only to certain classes of adsorbate-substrate systems. It is also an indirect method which often requires extensive data analysis. Furthermore, SEXAFS and LEED are area-averaging techniques and, as such, are relatively insensitive to low densities of atomic-scale disorder.

Currently, there is much interest in the interaction of column-V elements with Si substrates. This interest is driven in part by the desire to improve the quality of III-V epitaxy on Si. In addition to its current technological relevance, we have chosen the Si(100)2×1-Sb sur-

face for our combined SEXAFS and STM study since adatom-adatom near-neighbor bonding poses a challenging problem for either structural probe used in this work.^{3,5} As will be demonstrated, by combining both the short-range order derived from SEXAFS with the long-range order provided by STM, a complete experimental structural determination of this complex interface is possible. This surface structure can now be used to test the accuracy of theoretical calculations for metal/semiconductor interfaces.

The Si wafer samples were initially degassed for 6 h at 600 °C. The Si was then cleaned by heating to a temperature of 1150 °C for 15 min after which sharp two-domain 2×1 LEED patterns were observed. All temperatures were measured with an infrared pyrometer. Pressures during the sample heating did not exceed 1.5×10^{-9} Torr. For the STM measurements, between 0.6 to 2 monolayers (ML) of Sb were deposited at 375 °C. During deposition, the chamber pressure was in the 10^{-10} -Torr range. LEED showed a 1×1 pattern with diffuse, two-domain 2×1 spots. This sample-preparation technique had previously been reported to desorb all but 1 ML of Sb.⁶

A limited amount of imaging was done on samples annealed at 375 °C. These samples were found to be disordered, the images being similar to those reported by Rich *et al.*⁶ In order to obtain an ordered Sb overlayer, it was necessary to anneal the surface at 550 °C for 15 min, which showed a similar LEED pattern. As a result, all STM and SEXAFS data discussed are from samples annealed at 550 °C. The STM images were obtained in a UHV chamber, which has been described elsewhere,⁷ housing the STM, LEED optics, evaporation sources, and an electron-beam heater. The image shown below is for 0.6-ML coverage.

The SEXAFS data were recorded using the "JUMBO" double-crystal monochromator⁸ at the Stanford Synchrotron Radiation Laboratory (SSRL). The energy resolution was ~ 2 eV at a photon energy of 4100 eV using a pair of Ge(111) crystals. The experimental chamber (base pressure better than 7×10^{-11} Torr) consists of a main chamber equipped with LEED optics, a load-lock system, and a double-pass cylindrical mirror analyzer (CMA), the axis of which lies along the polarization vector of the synchrotron radiation. The sample manipulator has an on-axis configuration which allows the sample normal to be rotated in the plane formed by the CMA axis and the direction of light propagation. Samples were prepared in an adjacent chamber equipped with an electron-beam heater, Sb sources, and a quartz-crystal rate monitor.

The sample preparation for the SEXAFS experiment was similar to that for the STM samples with an initial Sb coverage of 2 ML. Auger electron spectroscopy determined the sample, both before and after Sb deposition, to be free of contamination. Sb L_3 edge ($E \sim 4130$ eV) SEXAFS were collected by monitoring the Sb $L_3M_{4,5}M_{4,5}$ Auger emission ($E \sim 3017$ eV) as a function of incident photon energy and flux in the constant final-state mode.⁹ Data were recorded at three different angles: glancing incidence (polarization vector and surface normal forming an angle of 15°), magic angle (polarization vector and surface normal forming an angle of 55°), and normal incidence (polarization vector and surface normal forming an angle of 75°).

Annealing samples with 0.6–2.0-ML initial Sb coverage at 550°C produced ordered surfaces such as that shown in Fig. 1. This image, $50 \text{ \AA} \times 50 \text{ \AA}$, was obtained at 0.6-ML Sb coverage; therefore some portion of the Si surface remains uncovered. The primary features of the

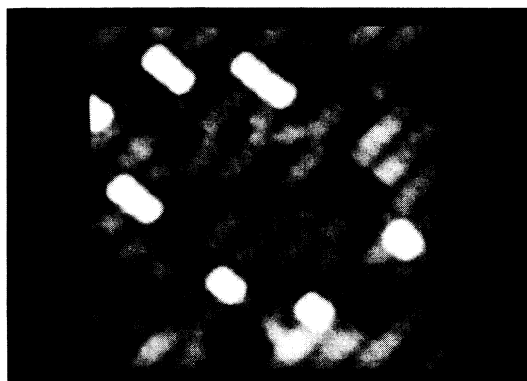


FIG. 1. A $50\text{-\AA} \times 50\text{-\AA}$ image of the unoccupied states of the $\text{Si}(001)2 \times 1$ -Sb surface annealed at 550°C . The Sb dimers are clearly seen. The brighter areas are Sb dimers of the second Sb layer. The dark regions correspond to bare Si. Also seen are antisite domain boundaries. The image was obtained in constant-current mode.

image are small oblong units whose dimensions are consistent with Sb dimers. The brighter features correspond to dimers lying one level above the majority, and the dark regions correspond to the level below which is bare Si.

This image is similar to images of the arsenic-terminated $\text{Si}(001)$ surface obtained by Becker, Klitsner, and Vickers,¹⁰ where the surface is entirely covered by As dimers. The principle difference is that the Sb-covered surface has a higher density of defects—either voids or antiphase defects—that break up the 2×1 ordering. Although the density of voids decreases somewhat at higher Sb coverages, the antiphase boundaries remain. As a result, the average coherence length of the Sb 2×1 reconstruction is below 50 \AA which accounts for

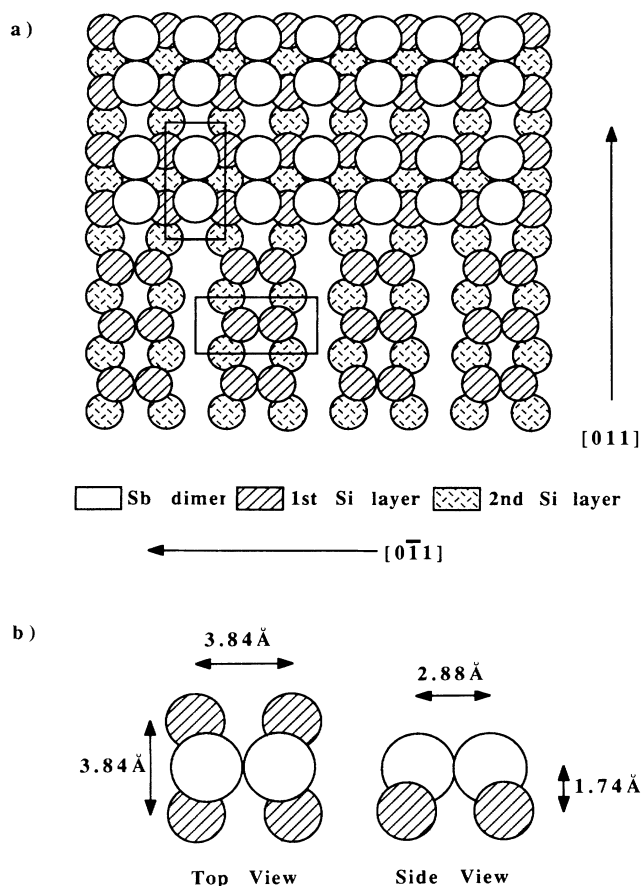


FIG. 2. (a) The registry of the Sb dimers observed by STM relative to the clean, unreconstructed $\text{Si}(001)2 \times 1$ surface. The dimers are aligned along the $[011]$ direction forming rows that run in the $[0\bar{1}1]$ direction. The rectangles show a single dimer in the surface unit cell. The dimensions of the rectangles are $3.84 \text{ \AA} \times 7.68 \text{ \AA}$. (b) The structure of a single Sb dimer. The atoms are drawn to scale with the radius of each atom taken to be the covalent radius in bulk Sb and Si. The bond lengths, registry, and chemical identification were determined by SEXAFS.

the diffuseness of the 2×1 spots in the LEED patterns seen from these samples. From the STM images, we infer that the Sb/Si(001) surface is comprised of dimers which form an ordered overlayer, as shown in Fig. 2(a). We must note, however, that the STM does not determine bond lengths, coordination, registry, or the chemical species of the atoms which form the dimers. SEXAFS can determine all of these undetermined quantities and lead to the complete description of this surface geometry.

For initial states of s symmetry (K and L_1 edges) the dipole selection rule dictates that the final state of an absorption process have p symmetry. However, states of initial p symmetry (L_2 or L_3 edges) can have both s or d final states. Stohr and Jaeger¹¹ have shown that the consequences of multiple final states can lead to inaccurate bond lengths and misleading coordination numbers. They have also shown that there is a magic angle, 54.7° from glancing incidence, at which $L_{2,3}$ -edge theory is formally equivalent to the K - or L_1 -edge case. Because of this equivalence, SEXAFS data obtained at the magic angle do not suffer from these additional errors. The bond lengths quoted in this work were therefore extracted from the magic-angle data.

The Fourier transforms of the grazing and normal incidence L_3 SEXAFS spectra are shown in Fig. 3. The best fit to the data was obtained by assuming that the peak at 2.1 \AA arises from Si backscattering and the peak at 3.2 \AA arises from Sb backscattering. The peak at 1.2 \AA is due to truncation effects caused by the limited k -space range of data. The peak at 4 \AA was not used in the data analysis; it corresponds to a combination of higher shell frequencies and truncation effects. The decrease in the peak amplitude at 2.1 \AA as the incidence angle is varied from grazing to normal incidence is evidence that the Sb-Si bond has an appreciable component normal to the surface.¹¹ The opposite behavior of the peak at 3.2 \AA shows that the Sb-Sb bond resides parallel to the surface plane.

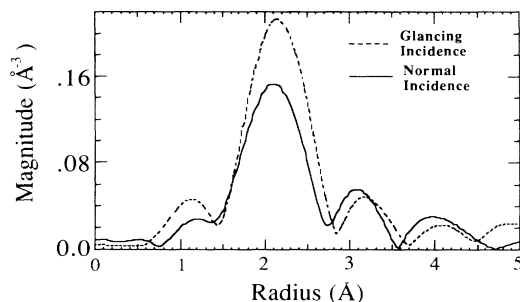


FIG. 3. The Fourier transforms of the k^2 -weighted Sb L_3 SEXAFS spectra for both glancing (dashed line) and normal (solid line) incidence. The angular dependence of the peaks at 2.1 and 3.2 \AA shows that the Sb-Si bond has a large component normal to the surface and that the Sb-Sb bond resides parallel to the surface plane.

A window function was used to isolate the contributions to the Fourier transform of the magic-angle SEXAFS from Si to Sb nearest neighbors. This portion of the Fourier spectrum was then backtransformed and a two-shell fit applied. The raw data, backtransform, and fit are shown in Fig. 4. Figure 4(a) shows that most of the signal is derived from the first shell which contains both Sb and Si backscattering. Figure 4(b) shows the accuracy of the fit. Crystalline AlSb was used as the phase standard for the Sb-Si bond, and Sb metal was used as the standard for the Sb-Sb bond. The Sb-Si bond length is determined to be $2.63 \pm 0.04 \text{ \AA}$, which is equivalent to the sum of the covalent radii of Si and Sb. The Sb-Sb bond length is determined to be $2.88 \pm 0.03 \text{ \AA}$, which is equivalent to that of bulk Sb.

In order to determine the bonding geometry, one must compare the effective coordination numbers to theoretical values for different adsorption sites. The effective $L_{2,3}$ coordination numbers as a function of angle for several models along with the experimental values are listed in Table I. The three adsorption models selected were chosen because, although two of the models do not contain Sb-Sb bonding, they correspond to monolayer coverages in which all dangling bonds are saturated. Partially filled bonds are unfavorable since they increase the surface energy. As demonstrated by Table I, the modified bridge site⁵ is supported by the SEXAFS experiment. This analysis therefore determines that the dimers observed by STM are comprised of Sb atoms each of which is bonded to two Si atoms. In this geometry, the Sb atoms reside $1.74 \pm 0.05 \text{ \AA}$ above the Si surface.

The modified bridge model is also consistent with photoemission studies of the Sb/Si(001) surface.¹² This

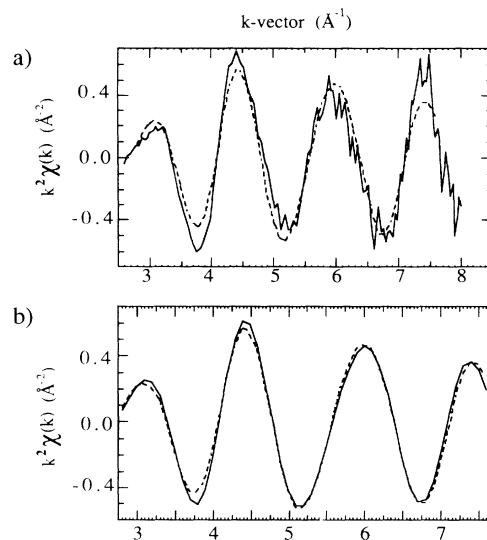


FIG. 4. (a) The raw k^2 -weighted Sb L_3 SEXAFS spectrum (solid line) and the backtransformed (Fourier filtered) data (dashed line) superimposed. The backtransform contains both the Sb and Si nearest-neighbor contributions. (b) The fit (solid line) with the backtransform (dashed line).

TABLE I. Comparison between the experimental Sb L_{3} effective coordination numbers and theory for three possible adsorption sites. The fourfold hollow site is roughly in the plane of the topmost Si layer and has fourfold Si coordination. The bridge site is an ideal bulklike termination of the Si surface. The modified bridge site consists of two Sb atoms in roughly the same location as for the bridge, but displaced towards each other to form a dimer.

Incidence	Expt.	Fourfold hollow	Bridge	Modified bridge
Antimony-silicon coordination				
Glancing	2.5 ± 0.4	5.21	2.17	2.35
Magic angle	3.1 ± 0.4	3.99	2.52	2.70
Normal	3.6 ± 0.4	2.97	2.50	2.41
<u>Glancing</u>	0.7 ± 0.2	1.75	0.87	0.93
Normal				
Antimony-antimony coordination				
Glancing	1.0 ± 0.2	0.00	0.00	1.20
Magic angle	1.1 ± 0.2	0.00	0.00	1.00
Normal	0.7 ± 0.2	0.00	0.00	0.73
<u>Glancing</u>	1.5 ± 0.2	1.53
Normal				

study failed to detect a surface component in the Si $2p$ core-level spectrum which implies that the Si has a nearly bulklike termination. The study also inferred that each Sb atom bonds to two Si atoms, in accord with our measurements. Angle-resolved photoemission,¹³ x-ray standing wave,¹⁴ and STM (Ref. 10) studies of the 1-ML As/Si(001) system conclude that As dimers occupy a similar bridge site. Our data therefore establish an interesting trend in the adsorption geometry of column-V elements on Si(001).

In order to determine the orientation of the Sb dimers relative to the Si substrate, LEED was performed on clean and Sb-covered vicinal Si(001) cut 4° towards the $\langle 110 \rangle$ direction. Vicinal Si has been shown to produce a single-domain stepped surface where each terrace is bordered by a step two atoms high resulting in a single-domain 2×1 LEED pattern. The LEED pattern obtained from the Sb-covered vicinal surface showed the 2×1 spots to be rotated 90° when compared to the LEED pattern obtained from the clean vicinal surface. This finding demonstrates that the Sb dimers run perpendicular to the Si dimers of the clean Si(001) 2×1 surface.

To summarize, by using a combination of SEXAFS and STM, we have determined the bonding geometry of the Si(001) 2×1 -Sb surface. Bond lengths, coordination, and registry were all determined experimentally. The Sb-Si bond length was found to be $2.63 \pm 0.04 \text{ \AA}$, and the Sb-Sb bond length was found to be $2.88 \pm 0.03 \text{ \AA}$. Each Sb atom was found to have one Sb and two Si near neighbors. Numerous antisite domains were observed with a typical domain dimension of $30 \text{ \AA} \times 30 \text{ \AA}$. The diffuseness of the 2×1 spots in the LEED pattern is explained by this small domain size. LEED on vicinal Si

shows that the Sb dimers run perpendicular to the original Si dimers of the clean Si(001) 2×1 surface.

Additionally, this work demonstrates the complimentary nature of SEXAFS and STM. Each technique supplements the other, supplying information that is inaccessible when each technique is used alone. The STM provides atomic-resolution information about the overlayer geometry on a size scale that is unattainable with SEXAFS. The real-space images also provide information about defect densities that are only indirectly measurable, if at all, with area-averaging techniques. SEXAFS provides the accurate bond lengths and chemically specific coordination unattainable with the STM. The two techniques make possible a complete experimental determination of interfacial structure.

This research was performed at SSRL which is operated by the Department of Energy, Office of Basic Energy Science, Division of Chemical Sciences. P.P. and I.L. acknowledge the support of that Office's Division of Material Sciences for this research. M.R. acknowledges support from the Stanford University Center for Materials Research under NSF-Materials Research Laboratory Grant No. DMR 87-217359. K.E.M., T.K., and W.E.S. acknowledge the support of Defense Advanced Research Projects Agency and ONR Contract No. N00014-89-J-1083. J.C.W. and C.E.B. acknowledge the support of NIST. J.N. and C.F.Q. acknowledge the support of the Office of Naval Research Contract No. N00014-90-J-1001. A.A.B. acknowledges the support from AT&T.

¹G. Binnig, H. Rohrer, Ch. Gerber, and E. Weibel, Phys. Rev. Lett. **49**, 57 (1982).

²P. Mårtensson and R. M. Feenstra, Phys. Rev. B **39**, 7744 (1988).

³D. K. Biegelsen, R. D. Bringans, J. E. Northrup, and L. E. Swartz, Phys. Rev. Lett. **65**, 452 (1990).

⁴P. H. Citrin, J. Phys. (Paris) **47**, 437 (1986).

⁵J. C. Woicik, T. Kendelewicz, K. E. Miyano, C. E. Bouldin, P. L. Meisner, P. Pianetta, and W. E. Spicer, Phys. Rev. B (to be published).

⁶D. H. Rich, F. M. Leible, A. Samsavar, E. S. Hirschhorn, T. Miller, and T.-C. Chiang, Phys. Rev. B **39**, 12758 (1989).

⁷S. Park and C. F. Quate, Rev. Sci. Instrum. **58**, 2010 (1987).

⁸J. Cerino, J. Stohr, and N. Hower, Nucl. Instrum. Methods **172**, 227 (1980).

⁹G. J. Lapeyre and J. Anderson, Phys. Rev. Lett. **35**, 117 (1975).

¹⁰R. S. Becker, T. Klitsner, and J. S. Vickers, J. Microsc. **152**, Pt. 1, 157 (1988).

¹¹J. Stohr and R. Jaeger, Phys. Rev. B **27**, 5146 (1983).

¹²D. H. Rich, T. Miller, G. E. Franklin, and T.-C. Chiang, Phys. Rev. B **39**, 1438 (1989).

¹³R. I. G. Uhrberg, R. D. Bringans, R. Z. Bachrach, and J. E. Northrup, Phys. Rev. Lett. **56**, 520 (1986).

¹⁴J. Zegenhagen, J. R. Patel, B. M. Kincaid, J. A. Golovchenko, J. B. Mock, P. E. Freeland, R. J. Malik, and K. G. Huang, Appl. Phys. Lett. **53**, 252 (1988).

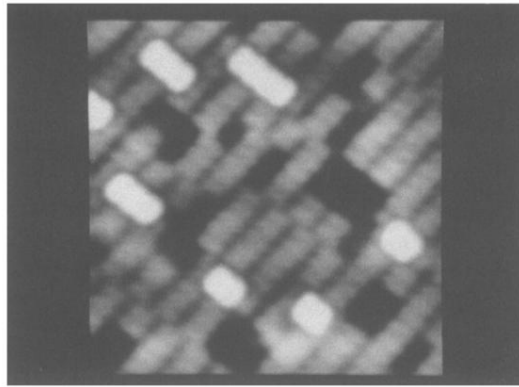


FIG. 1. A $50\text{-}\text{\AA} \times 50\text{-}\text{\AA}$ image of the unoccupied states of the $\text{Si}(001)2 \times 1\text{-Sb}$ surface annealed at 550°C . The Sb dimers are clearly seen. The brighter areas are Sb dimers of the second Sb layer. The dark regions correspond to bare Si. Also seen are antisite domain boundaries. The image was obtained in constant-current mode.

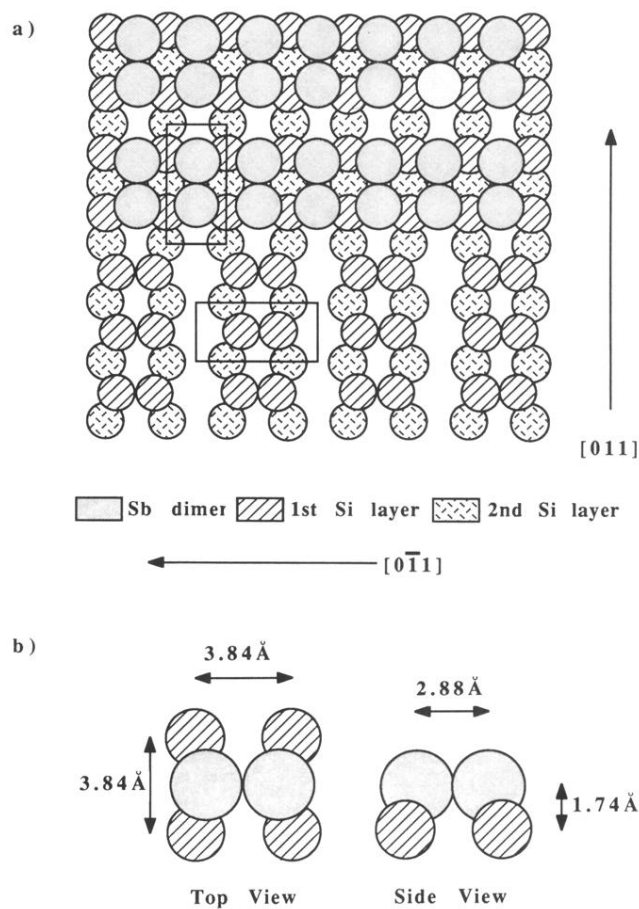


FIG. 2. (a) The registry of the Sb dimers observed by STM relative to the clean, unreconstructed Si(001) 2×1 surface. The dimers are aligned along the [011] direction forming rows that run in the $[0\bar{1}1]$ direction. The rectangles show a single dimer in the surface unit cell. The dimensions of the rectangles are $3.84 \text{ \AA} \times 7.68 \text{ \AA}$. (b) The structure of a single Sb dimer. The atoms are drawn to scale with the radius of each atom taken to be the covalent radius in bulk Sb and Si. The bond lengths, registry, and chemical identification were determined by SEXAFS.